Faculty of Graduate Studies
University of Jaffna

Smart Cement Behavior with Aggregates, Silicate, Clay, Carbon Dioxide and Real-Time Monitoring Characterized Using Vipulanandan Models

Vipulanandan C.[1],✉

[1] Professor of Civil and Environmental Engineering, Director, Center for Innovative Grouting Material and Technology (CIGMAT) and Director, Texas Hurricane Center for Innovative Technology (THC-IT), University of Houston, Houston, Texas 77204-4003.

✉ Corresponding author: CVipulanandan@uh.edu

Abstract:

Chemo-thermo-piezoresistive smart cement is a highly sensing binder that was recently developed to be used in multiple infrastructure applications in new constructions and also integrated into in-service infrastructures for real-time monitoring. In this study, the effects of up to 75% aggregates (representing concrete), 0.3% silicate, 5% clay (inorganic contamination) and 3% carbon dioxide (CO_2) on the curing and compressive piezoresistive behavior of the smart cement with less and 0.1% well dispersed carbon fibers was investigated. Also, the effect of temperature on the smart cement with silicate additive was investigated. A new material characterization method has been developed and was used to identify the critical electrical property of the smart cement with aggregates and other additives and the electrical resistivity was identified as the critical property to monitor. Hence a two-probe method was developed to monitor the resistivity changes in the cement. The piezoresistive axial strain at peak stress for the concrete with smart cement was over hundred percent which is 336 times (33,600%) higher compared to the concrete failure strain of 0.3%. The effects of silicate, clay and carbon dioxide on the initial resistivity (quality of mixing), temperature and compressive piezoresistivity have been quantified using Vipulanandan Models. It is important to monitor the real material property changes in the field and not just the temperature which is not a material property. A new approach has been developed to wirelessly transfer the two probes monitoring of the changes in resistivity of smart cement, smart concrete, regular cement and concrete to the phone and computers.

1. INTRODUCTION

Cement is an inorganic binding material and has evolved over 5,000 years from natural materials to industrial production with changes in the chemical compositions and the particle size distributions. Natural cement made from limestone containing clay minerals was continued to be used until the nineteenth century. When water is added to the cement, the cement will react with the water and bind with many types of inorganic materials to form durable composites for various types of applications. Historically cement is the most valuable material developed by humans to enhance the growth and developments around the world. Initially cement was used in the building of Egyptian pyramids. Also around 300 BC, Romans used cement with various types of admixtures to construct many types of buildings. The main focus over centuries has been on developing stronger and durable cements. In 1824, Portland cement was invented by Joseph Aspdin from Leeds, England. In the 1850s Vicat from France developed the Vicat needle method to determine the setting time of cement and this method is still being used. In America, the production of natural cements reached its peak in the 1890s, only to be overtaken by the Portland cement production. Now there are standards set for various types of Portland cements and oil well cements to ensure quality of production and also help with the multiple applications for cement. Cement is the largest manufactured material around the world and in recent years over 4 trillion Mega grams are being manufactured annually.

During the past 200 years cement and concrete have been widely used in many applications and has been well documented. Cement slurries and grouts, based on the water-to-cement ratio, have been used in the construction of shallow and deep oil, gas and water wells both onshore and offshore. Also cement slurries are used to bond the pipes to the formation in horizontal directional drilling. Cement slurries are used to bond the steel casings and pipes to the varying geological formations in the wellbore and also to isolate the formations. In the well application cement has to

bond very well with the highly varying natural geological formations with depth and to the human made steel casing and pipes and also has to perform for many decades under varying loading conditions, temperatures, pressures and seismic activities. Hence it is important to monitor the performance of the cement from the time of mixing to the entire service life in-situ (Vipulanandan 2021).

1.1 Cements

Cement is manufactured by combining clay or shale (aluminum silicate) with limestone (calcium based) and processed around 1450^0C or higher temperatures to produce the calcium silicate clinkers. At present cements are broadly characterized based on the applications as Portland cements and oil well cements.

1.1.1 Portland Cement

The first American Society for Testing and Materials (ASTM) Portland Cement standard was developed in 1940. Now the ASTM C150/C150M-19 covers ten types of Portland cements based on the applications and compositions. Type I is the general-purpose cement used for construction purposes and together with Type II, accounts for about 92% of the United States produced cement. Type III only accounts for about 3.5% of cement production, while Type IV is only available on special request and Type V is difficult to obtain because of less than 0.5% of production.

1.1.2 Oil Well Cement (OWC)

When used in oil wells, the cement has multiple functions which includes structural integrity, protective seal to the casing, preventing blowout and to promote zonal isolation. Portland cement was used in the oil well construction in 1906. In 1948, American petroleum Institute (API) developed the first code for testing cement. The standards of API suggest adopting the chemical requirements determined by the ASTM procedures and physical requirements determined in accordance with procedures outlined in API RP 10B and ASTM. Based on the API classification, currently there are six classes of cements (classes A, B, C, D, G and H) which could be used for oil well cementing based on the depths and downhole pressures and temperatures.

Cement slurry flowing ability (rheology) and stability are two of the major requirements of oil well cementing. Oil-well cements (OWCs) are usually made from Portland cement clinker or from blended hydraulic cements. OWCs are classified into grades by the API based upon there $Ca_3Al_nO_p$ (Tricalcium Aluminate – C_3A) content as Ordinary (O), Moderate Sulphate Resistant (MSR), and High Sulphate Resistant (HSR). Each class is applicable for a certain range of well depth, temperature, pressure, and sulphate environments.

1.2 Smart Cement

It is important to make the cement highly sensing to monitor the changes in the stresses, cracking, temperature, erosion and also contamination during its service life. Chemo-thermo-piezoresistive smart cement using Portland cement and oil well cement have been recently developed (U.S. Patent 10,481,143 (2019) Inventor Vipulanandan) which can sense

and real-time monitor the many changes happening inside the cement during cementing of wells to concreting of various infrastructure to the entire service life of the structures. In concrete smart cement is the binder which can sense the changes within the concrete. The smart cement can sense the changes in the water-to-cement ratios, different additives, contamination and pressure applied to the cement sheath or concrete in terms of chemo-thermo-piezoresistivity. The failure compressive strain for the smart cement was 0.2% at peak compressive stress and the resistivity change is of the order of several hundred percentage making it over 500 times (50,000%) more sensitive (Vipulanandan et al. 2014-2021).

1.2.1 Piezoresistive Behavior

The change of electrical resistance in metal devices due to an applied mechanical load was first discovered in 1856 by Lord Kelvin. With single crystal silicon becoming the material of choice for the design of analog and digital circuits, the large piezoresistive effect in silicon and germanium was first discovered in 1954 (Smith 1954).

Usually, the resistance change in metals is mostly due to the change of geometry resulting from applied mechanical stresses. However, even though the piezoresistive effect is small in those cases it is often not negligible. Strain gages are good example of a piezoresistive material where with the application of strain to the attached material the electrical resistance will change in the strain gages because how the metal strain gages are configured. Also in the strain gages the resistance change will be positive under tensile stress or strain and negative under compressive stress or strain. In the past few decades various investigations have been performed to make the polymers and cement composites to be piezoresistive (Chung et al. 1995, 2000 and 2001; Vipulanandan et al. 2002, 2005-2008). In the recently developed smart cement by Vipulanandan (U.S. Patent Number 10,481,143 (2019)) the resistivity change is positive under both tensile and compressive loading because the changes are dominated by the deviatoric (shear) stresses in the cement (Vipulanandan et al. 2014-2021).

1.2.2 Thermo-resistive Behavior

In the sensing element electrical resistance will change due to temperature change in the operating temperature ranges. In 1871, platinum was proposed by Sir William Siemens to be the most suitable material (Siemens, 1871). Also nickel and copper have been developed to temperature sensors due to measurable changes in electrical resistance. Recently develop smart cement by Vipulanandan also can be used to sense the temperature changes due to measureable changes in electrical resistivity (Vipulanandan et al. 2014b).

1.2.3 Chemo-resistive Behavior

Chemo-resistive materials are a class of sensors that changes in electrical resistance in response to the changes in the surrounding chemical environment. Materials such as metal oxide semiconductors, conductive polymers and nano materials like graphene, carbon nanotubes and nanoparticles. As far back as 1965, there are reports on semiconductor materials exhibiting electrical resistivity changes due to ambient gases and vapors. In 1985, Wohltjen and Snow developed a copper compound to detect ammonia vapor at

room temperature and the resistivity decreased (Wohltjen et al. 1985). Recently develop smart cement by Vipulanandan also can be used to sense the chemical additives and contaminations based on the changes in the electrical resistivity (Vipulanandan et al.2014b, 2018k).

1.3 Behavior Models

It is important to have behavior models for cements and concretes to not only clearly understand the behavior but also to integrate it with the artificial intelligent (AI) networks and 3D printing applications. The past models developed for cement hydration and cement behavior under various loading conditions are empirical and limited to the ranges of variables investigated in the relevant studies. In concrete, cement is the binder that develops the strength and other relevant properties for the concrete. But the behavior models do not quantify the role of cement in the concrete. Recently a new Vipulanandan rheological models has been developed to better characterize the rheological behavior of the smart cement slurry, drilling muds, spacer fluids and other fluids with and without various additives including nanoparticles (Afolabi et al. 2019; Tchameni, et al. 2019; Montes 2019; Mohammed 2018; Vipulanandan et al. 2014a). Also, analytical models have been developed to characterize the curing, stress-strain and piezoresistive behaviors of the smart cement (Vipulanandan et al., 1990-2021). The Vipulanandan fluid flow model (generalized Darcy's model) and fluid loss model have been developed and verified with experimental results. Also new Vipulanandan failure model for cement and concrete has been developed and verified with experimental test results.

2. OBJECTIVE

The overall objective was to highlight the potential use of the highly sensing smart cement integrated with real-time monitoring in new and also in-service infrastructures. The specific objectives are as follows:

1) Evaluate the smart cement curing and compressive piezoresistive behaviour with aggregates, silicate, clay contamination and carbon dioxide
2) Develop real-time monitoring applications in new constructions including concrete based constructions, deep oil wells, deep foundations and other infrastructures.
3) Developing real-time monitoring methods to integrate the smart cement blocks into in-service infrastructures.

3. MATERIALS AND METHODS

In this study chemo-thermo-piezoresistive smart cement (Vipulanandan et al. 2014-2021; Vipulanandan 2021) was used to develop the concrete (aggregates) and also smart cement with few selected additives. For the curing and compressive behavior studies samples were cast in plastic cylindrical molds with diameter of 50 mm and a height of 100 mm. Two conductive wires were placed in all of the molds to measure the changing in electrical resistivity. At least three specimens were tested under each condition investigated in this study.

3.1 Materials

3.1.1 Sample Preparation

In this study table top blenders were used to prepare the cement and concrete specimens (CIGMAT Standards 2002-2006).

Smart cement (sensing cement):
Cement was mixed with 0.1% carbon fibers to make it piezoresistive material (Vipulanandan et al., 2014a, b; 2015a, b).

Smart Cement Concrete
Smart cement concrete specimens were prepared using smart cement (less than 0.1% carbon fibers) with water-cement ratio of 0.38 (Vipulanandan et al. 2018c). Concrete specimens were prepared using 75% coarse aggregates based on the total volume of concrete. Sieve analysis (ASTM C136) was performed to determine the particle size distribution of the aggregates. The median diameter, which also represents d_{50} (ASTM) the size of 50% of the aggregates was less than 4.2 mm. After mixing, the concrete was placed in 100 mm height and 50 mm diameter cylindrical molds with two conductive flexible wires 1 mm in diameter (representing the probes) were placed 50 mm apart vertically to measure the electrical resistance. The specimens were cured up to 28 days under relative humidity of 90%. At least three specimens were test under each condition and the average values are presented in the figures, tables and discussion.

Smart Cement with Additives
After preparing the smart cement different additives were added in varying amounts and mixed for at least 3 minutes before placing them in the wired molds. At least three specimens were test under each condition and the average values are presented in the figures, tables and discussion.

3.2 Methods

3.2.1 Electrical Resistivity

Two different devices were used to measure the changes in the electrical resistivity of concrete and grout immediately after mixing up to the time they solidify. Both of the electrical resistivity devices were calibrated using the standard solutions of sodium chloride (NaCl).

Conductivity Probe
A commercially available conductivity meter was used to measure the conductivity (inverse of electrical resistivity). The conductivity measuring range was from 0.1μS/cm to 1000 mS/cm, representing a resistivity of 100,000 Ω.m. to 0.01 Ω.m. respectively.

Digital Resistivity Meter:
The digital resistivity meter measured the resistivity in the range of 0.01Ω-m to 400 Ω-m.

3.2.2 Electrical Resistance

LCR meter (inductance (L), capacitance (C), and resistance (R)) was used to monitor the electrical resistance of the specimens during the curing time. Two wire method with AC at 300 kHz frequency was used in order to minimize the contact resistances (Vipulanandan et al. 2013). During the initial stage of curing both the electrical resistivity (ϱ)

electrical resistance (R) were measured to determine the parameters K and G based on the Eqn.1.

$$\rho = \frac{R}{K+GR} \qquad (1)$$

In this study, electrical resistance (R) and electrical resistivity (ρ) were measured independently during the initial curing period and the effective calibration factors (K and G) for the materials used in this study (insulators) were determined experimentally. For the smart cement and concrete Parameter G = 0 and Parameter K became stable (constant) in two to three hours. The Parameter K was more than double than the nominal Parameter K_n equal L/A where L is the spacing between the measuring wires and A is the cross section for the specimens tested.

Normalized change in resistivity $\Delta\rho$ with the changing conditions can be represented as follows:

$$\frac{\Delta\rho}{\rho} = \frac{\Delta R}{R} \qquad (2)$$

The smart cement material is represented in terms of resistivity (ϱ) and the changes due to stress, temperature and added additive and contaminants will be quantified to evaluate the sensitivity of the material parameter resistivity.

Two Wire Method

The change in resistance was measured using the two probe method with the LCR meter. To minimize the contact resistances, the resistance was measured at 300 kHz using two-wire method. This configuration was first calibrated using the same liquid (cement slurry) to determine the parameter K in Eqn. (1).

3.2.3 Compression Test (ASTM C39)

The cylindrical specimens (concrete, cement and grout) were capped and tested at a predetermined controlled displacement rate. Tests were performed using the Tinious Olsun machine at a controlling the displacement rate to 0.125 mm per minute (CIGMAT 2002). In order to measure the strain, a commercially available extensometer (accuracy of 0.001% strain) was used. During the compression test, the change in resistance was measured continuously using the LCR meter. Two probes method with alternative current (AC) at 300 kHz frequency was used in order to minimize the contact resistances (Vipulanandan and Amani, 2018c). The change in resistance was monitored using the two-probe method, and the parameter in Eqn. (2) was used relate the changes in resistivity to the applied stress.

3.2.4 Modeling

Vipulanandan Curing Model

In order to represent the electrical resistivity development of the cement, Vipulanandan Curing model was used (Vipulanandan and Mohammed, 2015) and the relationship is as follows:

$$\frac{1}{\rho} = \frac{1}{\rho_{min}}\left[\frac{\left(\frac{t+t_0}{t_{min}+t_0}\right)}{q_1+(1-p_1-q_1)\left(\frac{t+t_0}{t_{min}+t_0}\right)+p_1\left(\frac{t+t_0}{t_{min}+t_0}\right)^{\left(\frac{p_1+q_1}{p_1}\right)}}\right] \qquad (3)$$

Where ρ is the electrical resistivity in Ω.m, ρ_{min} is the minimum electrical resistivity in Ω.m, t_{min} is the time corresponding to the minimum electrical resistivity (ρ_{min}), t represents the curing time, t_0 is the model parameter influenced by the initial resistivity and p_1 and q_1 are time-dependent model parameters.

Vipulanandan Piezoresistivity Model

In order to represent the piezoresistive behavior of the hardened cement, Vipulanandan Piezoresistivity Model (Vipulanandan et al., 2015, 2016) was used and the relationship is as follows:

$$\sigma = \frac{\sigma_{max}\times\left(\frac{\left(\frac{\Delta\rho}{\rho}\right)}{\left(\frac{\Delta\rho}{\rho}\right)_0}\right)}{q_2+(1-p_2-q_2)\times\left(\frac{\left(\frac{\Delta\rho}{\rho}\right)}{\left(\frac{\Delta\rho}{\rho}\right)_0}\right)+p_2\times\left(\frac{\left(\frac{\Delta\rho}{\rho}\right)}{\left(\frac{\Delta\rho}{\rho}\right)_0}\right)^{\left(\frac{p_2+q_2}{p_2}\right)}} \qquad (4)$$

Where σ_{max} is the maximum stress, $(\Delta\rho/\rho)_0$ is the piezoresistivity of the hardened cement under the maximum stress and p_2 and q_2 are model parameters influenced by the material properties.

3.2.5 Material Characterization

It is important to first characterize the materials based on the electrical properties, which can be easily adopted in the field.

Vipulanandan Impedance Model

Vipulanandan et al. (2013) studied different possible equivalent circuits for composite materials with two probes measurement and found appropriate equivalent circuits to represent materials.

CASE 1: General Bulk Material – Capacitance and Resistance

In the equivalent circuit for Case1, the contacts were connected in series, and both the contacts and the bulk material were represented using a capacitor and a resistor connected in parallel. In the equivalent circuit for CASE 1, R_b and C_b are resistance and capacitance of the bulk material, respectively; and R_c and C_c are resistance and capacitance of the contacts, respectively. Both contacts are represented with the same resistance (R_c) and capacitance (C_c), as they are identical. Total impedance of the equivalent circuit for Case 1 (Z_1) can be represented as:

$$Z_1(\sigma) = \frac{R_b(\sigma)}{1+\omega^2 R_b^2 C_b^2} + \frac{2R_c(\sigma)}{1+\omega^2 R_c^2 C_c^2} - j\left\{\frac{2\omega R_c^2 C_c(\sigma)}{1+\omega^2 R_c^2 C_c^2}+\frac{\omega R_b^2 C_b(\sigma)}{1+\omega^2 R_b^2 C_b^2}\right\} \qquad (5)$$

where ω is the angular frequency of the applied signal. When the frequency of the applied signal is very low, $\omega \to 0$, $Z_1 = R_b + 2R_c$, and when it is very high, $\omega \to \infty$, $Z_1 = 0$.

CASE 2: Special Bulk Material - Resistance Only

CASE 2 is a special case of CASE 1 in which the capacitance of the bulk material (C_b) is assumed to be negligible. The total impedance of the equivalent circuit for Case 2 (Z_2) is

$$Z_2(\sigma) = R_b(\sigma) + \frac{2R_c(\sigma)}{1 + \omega^2 R_c^2 C_c^2} - j\frac{2\omega R_c^2 C_c(\sigma)}{1 + \omega^2 R_c^2 C_c^2}. \quad (6)$$

When the frequency of the applied signal is very low, $\omega \to 0$, $Z_2 = R_b + 2R_c$, and when it is very high, $\omega \to \infty$, $Z_2 = R_b$ (Fig. 1).

The shape of the curves shown in Figure 1 is very much influenced by the material response and the two probes used for monitoring. Testing of smart cement and concrete indicated that CASE 2 represented their behaviors and hence the bulk material properties can be represented by resistivity and characterized at a frequency of 300 kHz using the two probes.
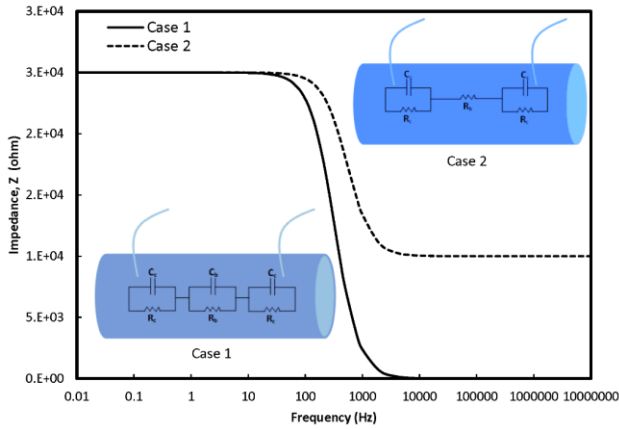

Figure 1. Vipulanandan impedance-frequency models for composite materials

It is important to identify the type of the testing material (example: metal, cement, concrete, plastic, wood, asphalt) so that the relevant material property can be measured and monitored in the field. Based on the past experience and research, changes in electrical properties were selected to be the representative properties for the cement and other materials so that it can be used for monitoring in multiple applications. Electrical properties of a material can be represented by the permittivity, resistivity or a combination being in number of series or parallel electrical circuits.

3.2.6 Statistical Parameters for Model Predictions

In order to determine the accuracy of the model predictions, both the root mean square error (RMSE) and the coefficient of determination (R^2) in curve fitting are defined in Eqns. (7) and Eqns. (8) as follows:

$$RMSE = \sqrt{\frac{\sum_{i=1}^{n}(y_i - x_i)^2}{N}} \quad (7)$$

$$R^2 = \left(\frac{\sum_i(x_i - \bar{x})(y_i - \bar{y})}{\sqrt{\sum_i(x_i - \bar{x})^2} * \sqrt{\sum_i(y_i - \bar{y})^2}}\right)^2 \quad (8)$$

where y_i = actual value; x_i = calculated value from the model; $\bar{y}$ = mean of the actual values; $\bar{x}$ = mean of the calculated values and N is the number of data points.

4. RESULTS AND ANALYSES - MATERIAL CHARACTERIZATION

4.1 Effect of Aggregates

4.1.1. Impedance Vs Frequency Relations

Investigation of the impedance versus frequency relationship tested immediately after mixing and also after 28 days of curing for the smart cement and smart cement concrete (75% aggregates) is shown in Figures 2 and 3. The observed shape of the curve represents the CASE 2, indicating that the bulk material can be represented by resistance. This has been verified for over 5 years.
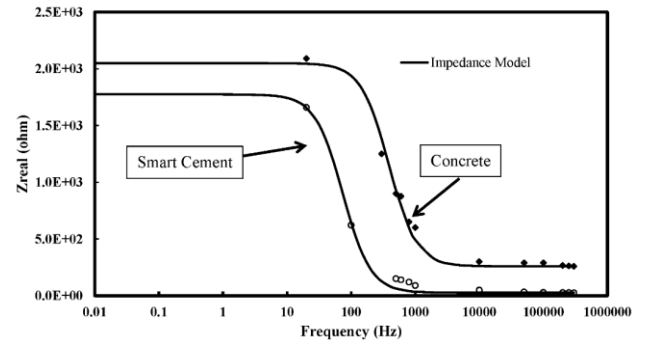

Figure 2. Impedance - Frequency Characterization of the Smart Cement and Concrete Immediately after Mixing
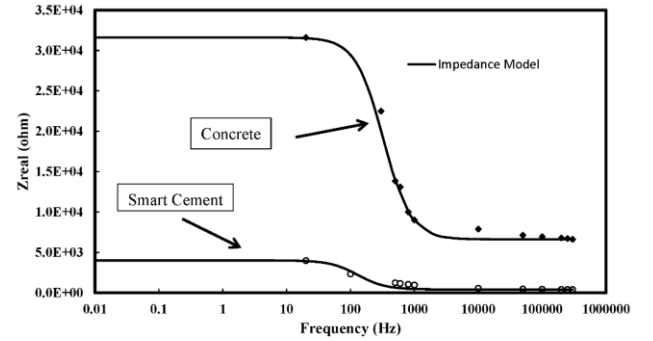

Figure 3. Impedance - Frequency Characterization of the Smart Cement and Concrete after 28 Days of Curing

Initial resistivity

Initial electrical resistivity increased with the addition of aggregates.

(a) Smart Cement:

The average initial electrical resistivity of the smart cement was 1.02 Ω.m.

(b) Smart Cement Concrete (with aggregate):

75% Gravel: The average initial electrical resistivity of the smart cement concrete with 75% gravel increased by 267% to 3.74 Ω.m. This increment was due to gravel content in the concrete.

5

4.1.2 Resistivity during curing

From the standpoint of conductivity, concrete can be regarded as a two-component composite material, pore solution and solid phase (aggregate + hydration products + unhydrated binders). During the setting of the cement, the capillary porosity is constant and changes in the pore solution resistivity leads to determine the evolution of the slurry resistivity. As shown in Figure 4, the pore resistivity decreased initially and reached a minimum resistivity of ρ_{min} at specific time of t_{min} which is due to increment of ionic concentration in pore solution. By preceding the hydration, production of Calcium Silicate Hydrate (C-S-H) network caused the increment in the paste resistivity (Zhang et al., 2010; Vipulanandan et al. 2015-2021).
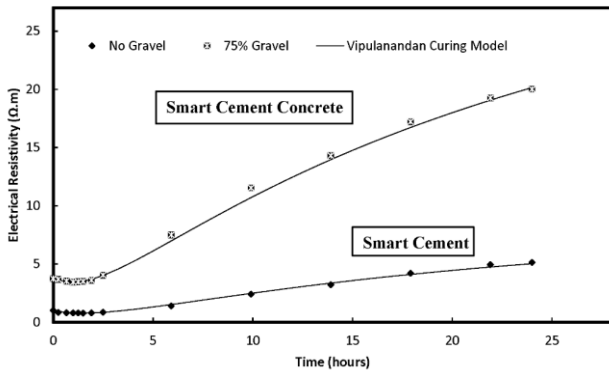

Figure 4. Development of electrical resistivity of smart cement composites during the initial 24 hours of curing
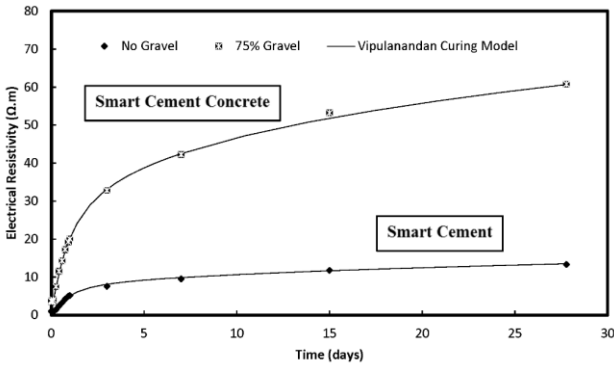

Figure 5. Development of electrical resistivity of smart cement composites during 28 days of curing

1 Day Curing

(a) Smart Cement:

The minimum electrical resistivity of the smart cement after 90 minutes of mixing was 0.79 Ω.m (Table 1, Figure 4).

(b) Smart Cement Concrete:

75% Gravel: The minimum electrical resistivity of the 75% gravel smart cement concrete increased by 339% to 3.46 Ω.m. The time corresponds to the minimum resistivity of 75% gravel smart cement concrete reduced by 30 minutes to 60 minutes compare to the smart cement.

28 Days Curing

(a) Smart Cement:

After 28 days of curing, the electrical resistivity of smart cement was 14.14 Ω.m. (Fig. 5).

(b) Smart Cement Concrete:

75% Gravel: After 28 days of curing the electrical resistivity of 75% gravel smart cement composite increased by 333% to 61.24 Ω.m.

4.1.3 Compressive Behavior

4.1.3.1 Compressive Strength

Compressive strength of smart cement and smart concrete were tested after 1 and 28 days of curing are summarized in Table 2.

1 day curing

(a) Smart Cement:

After 1 day of curing, the compressive strength of the smart cement was 8.6 MPa.

(b) Smart Cement Concrete:

75% Gravel: The compressive strength of the 75% gravel smart composite decreased by 29% to 6.1 MPa compare to the smart cement with no gravel.

28 days curing

(a) Smart Cement:

After 28 days of curing, the compressive strength of the smart cement was 21.7 MPa.

(b) Smart Cement Concrete:

75% Gravel: The compressive strength of the 75% gravel concrete decreased by 43% to 12.4 MPa compare to the smart cement with no gravel. Changes in compressive strength of the concrete can be justified with the percentage of cement in the concrete.

Table 1. Electrical resistivity parameters of the smart cement composites slurries

Smart Cement Concrete	ρ_0	ρ_{min}	t_{min}	ρ_{24}	$\dfrac{\rho_{24} - \rho_{min}}{\rho_{min}}$
(by volume)	(Ω.m)	(Ω.m)	(minutes)	(Ω.m)	%
No Gravel	1.02	0.79	90	5.14	550%
75% Gravel	3.74	3.46	60	20.01	478%

Table 2. Model parameters of p-q model for evaluating the piezoresistivity behavior of the concrete

Smart Cement Concrete	p_2	q_2	R^2	Compressive Strength (MPa)	Ultimate Piezoresistivity (%)	RMSE (MPa)
1 Day Curing						
No Gravel	0.61	0.57	0.99	8.6	375	0.3
75% Gravel	0.40	0.80	0.99	6.1	163	0.3
28 Days Curing						
No Gravel	0.83	0.42	0.98	21.7	204	1.0
75% Gravel	0.81	0.40	0.99	12.4	101	0.4

4.1.3.2 Piezoresistivity

Piezoresistive behavior of smart cement and smart cement concrete was evaluated after 1 day and 28 days of curing as shown in Figure 6.
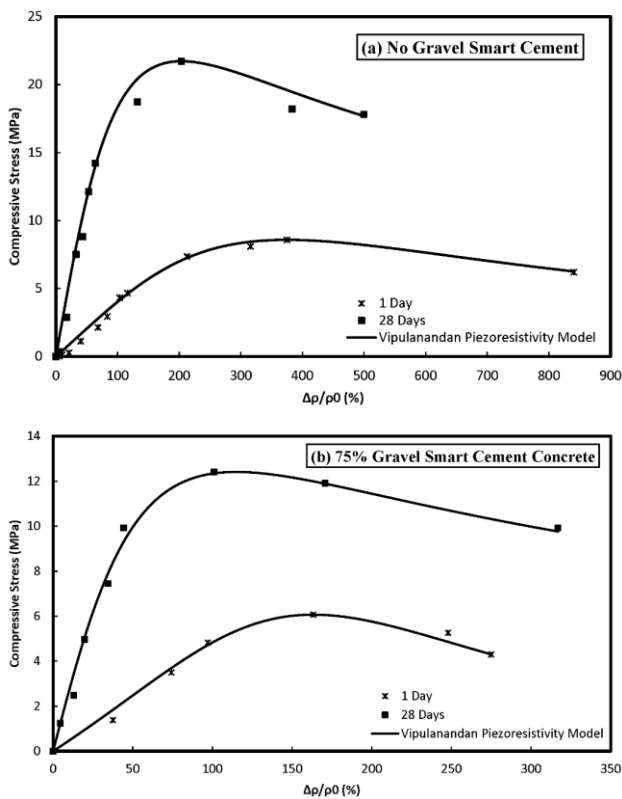

Figure 6. Piezoresistivity of smart cement composites after 1 and 28 days of curing: (a) No gravel and (b) 75% Gravel

1 day curing

(a) Smart Cement:

After 1 day of curing, the piezoresistivity of the smart cement at the peak compressive stress was 375% (Fig. 6. Table 2). Parameters p_2 and q_2 for the model were 0.61 and 0.57 respectively.

(b) Smart Cement Concrete:

75% Gravel: The piezoresistivity of the 75% gravel smart composite reduced by 57% to 163% compare to the smart cement. Parameters p_2 and q_2 for the model were 0.40 and 0.80 respectively.

28 days curing

(a) Smart Cement:

After 28 days of curing, the piezoresistivity of the smart cement was 204%. Parameters p_2 and q_2 for the model were 0.83 and 0.42 respectively.

(b) Smart Cement Concrete:

75% Gravel: The piezoresistivity of the 75% gravel smart composite reduced by 51% to 101% compare to the smart cement. Parameters p_2 and q_2 for the model were 0.81 and 0.40 respectively.

4.2 Effect of Sodium Meta Silicate (SMS)

Based on the applications and the environments, all types of standard cements are modified with various types of inorganic and organic additives (Vipulanandan et al. 1992, 2012 - 2021). Also during construction and service life of the structures constructed using cement based materials, contamination is also a possibility and hence investigating the sensitivity of smart cement to detect chemical, temperature and stress changes for real-time monitoring must be investigated. To minimize the delays during construction, failures and also safety issues, it is important to quantify the changes in the chemo-thermo-piezoresistive cement.

From the initial use in the late 1800's sodium silicate based compounds have been used in a number of applications including cementing, grouting, emulsifying, and in cleaning agents (Mbaba et al 1983). Of the various forms of sodium silicate based compounds, sodium meta-silicates (anhydrous) have been used in oil and gas industry and infrastructure repairing applications. Sodium meta-silicate (Na_2SiO_3; SMS) is a water-soluble powder, which is produced by fusing the silica sand with sodium carbonate at 1400°C (Nelson, 1990). Because of its emulsification and interfacial tension reduction characteristics, SMS has been used in alkaline flooding, a chemical recovery method to recover oil from various types of geological formations and sand. The overall objective of the study was to investigate the effects of adding varying amounts of SMS and higher temperature (80°C/176°F) curing on the piezoresistive behaviour of the smart cement with and without SMS.

4.2.1 Curing Methods

4.2.1.1 Room Condition

Specimens were cured in the plastic molds at room temperature (23°C) and a relative humidity of 50% and the specimens were demolded just before testing.

(b) Oven Cured

Specimens were kept in the plastic mold and cured in the oven at elevated temperature. Also specimens were placed in saturated sand in the closed bottle (Figure 7) to simulate the field condition under water and groundwater and cured at room temperature and elevated temperatures and were demolded just before testing.

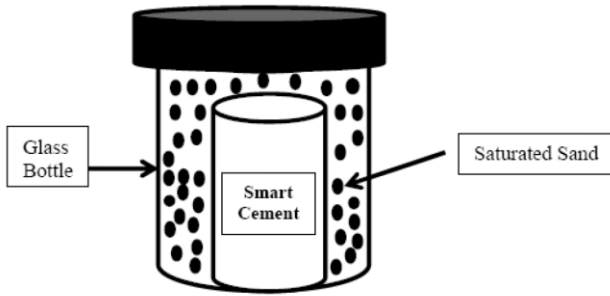Also, water was added regularly to keep the sand saturated.

Figure 7. Curing of Smart Cement Under Saturated Sand

4.2.2 Testing

Sodium meta-silicate (SMS) solution was characterized by determining the pH and the resistivity of the water solutions. With the addition of 0.1% SMS, the pH of water increased from 7.7 to 11.8, a 50% change in the pH. With the addition of 0.3% SMS the pH of the solution was 12.4, a 60% change. The resistivity of the tap water decreased from 27.0 Ω.m to 4.15 Ω.m with addition of 0.1% SMS, 85% reduction in resistivity. With the addition of 0.3% SMS the resistivity reduced to 2.0 Ω.m, 93% reduction.

4.2.2.1 Density

Adding SMS powder to the cement slurry (water-to-cement ratio of 0.40) slightly increased the density of the cement mixtures. Adding 0.3% SMS (by weight of water) to the cement slurry increased the density from 1.94 g/cm^3 (16.2 ppg) to 1.95 g/cm^3 (16.3 ppg) at room condition curing, 0.6% increase.

4.2.2.2 Initial Resistivity

The electrical resistivity of the cement slurry with and without SMS was measured immediately after mixing. The initial resistivity of the smart cement slurry was 0.97 Ω.m and it decreased with the addition of sodium metasilicate (SMS) as shown in Figure 8. With the addition of 0.1% SMS the resistivity decreased to 0.92 Ω.m, a 5% reduction. With the addition of 0.2% and 0.3% SMS the resistivity were 0.9 Ω.m and 0.88 Ω.m. Hence the resistivity was sensitive to the concentration of SMS in the cement. The resistivity was decreased to 0.8 Ω.m with 1% SMS which is a 17% decrease. Hence the resistivity is highly sensitive material property and

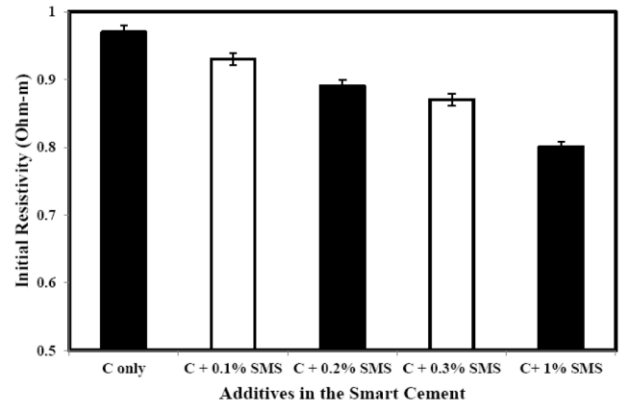will be good monitoring and quality control parameter in the field.

Figure 8. Initial Electrical Resistivity with Sodium Meta Silicate Addition

4.2.3 Compressive Piezoresistivity Behavior

With the addition of up to 0.3% SMS (inorganic additive), the tests showed that the smart cement cured under high temperature and different environments (dry and saturated sand) was a highly sensitive chemo-thermo-piezoresistive material.

1 day of curing

The compressive strength (σ_{cf}) of the smart cement after one day of curing at 80°C in the oven was 15.81 MPa which increased to 18.00 MPa when cured in the saturated sand at 80°C, a 14% increase. For smart cement with 0.3% SMS cured at 80°C had a compressive strength of 14.93 MPa which increased to 16.91 MPa when oven cured in saturated sand at 80°C, a 13% increase (Table 3).

The piezoresistive axial strain at failure $\left(\frac{\Delta\rho}{\rho_o}\right)_f$ for the smart cement air cured at 80°C was 433% and it increased to 475% for smart cement cured in saturated sand at 80°C. The smart cement with 0.3% SMS cured in oven showed the piezoresistive axial strain at failure $\left(\frac{\Delta\rho}{\rho_o}\right)_f$ was 331% and it increased to 345% when cured in saturated sand at 80°C (Table 3). The piezoresistivity at the peak compressive stress varied from 1555 to 2375 times the compressive strain of the smart cement.

Using the p-q Piezoresistive model (Eqn. (4)), the relationships between compressive stress and the piezoresistive axial strain $\left(\frac{\Delta\rho}{\rho_o}\right)$ of the smart cement with and without 0.3% SMS for one day of curing at 80°C in air and saturated sand were modeled. The piezoresistive model (Eqn. (4)) predicted the measured stress-piezoresistivity strain relationship very well as shown in Figure 9. The model parameters q_2 and p_2 are summarized in Table 3. The coefficients of determination (R^2) were 0.98 to 0.99. The root mean square of error (RMSE) varied between 0.11 MPa and 0.38 MPa as summarized in Table 3.

Table 3. Piezoresistivity model parameters for the smart cement with and without SMS cured at 80°C for 1 day of curing.

Composition and Curing Conditions	Curing Time (day)	Strength σ_{cf} (MPa)	Piezoresistive Strain at Peak Stress, $(\Delta\varrho/\varrho_o)_{cf}$ (%)	Model Parameter p_2	Model Parameter q_2	R^2	RMSE (MPa)
w/c=0.4, (Oven cured)		15.81	433	0.010	0.673	0.99	0.12
w/c=0.4, (Cured in Saturated Sand)		18.00	475	0.030	0.802	0.98	0.38
w/c=0.4, SMS=0.3% (Oven cured)	1 day	14.93	331	0.048	0.730	0.99	0.16
w/c=0.4, SMS=0.3% (Cured in Saturated Sand)		16.91	345	0.081	0.897	0.99	0.11

Table 4. Piezoresistivity model parameters for the smart cement with and without SMS cured at 80°C for 28 days of curing.

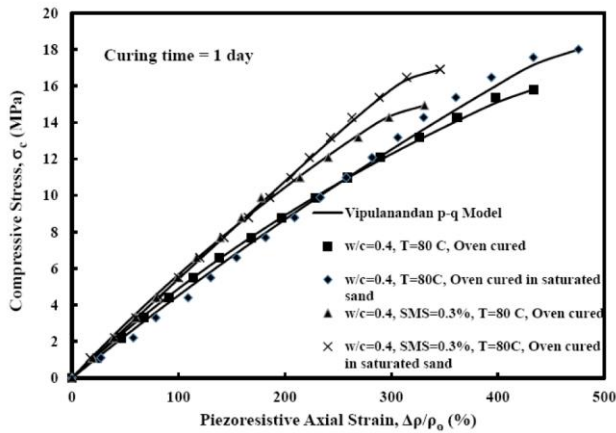| Composition and Curing Conditions	Curing Time (day)	Strength σ_{cf} (MPa)	Piezoresistive Strain at Peak Stress, $(\Delta\varrho/\varrho_o)_{cf}$ (%)	Model Parameter p_2	Model Parameter q_2	R^2	RMSE (MPa)
w/c=0.4, (Oven cured)		33.59	245	0.010	0.626	0.98	0.39
w/c=0.4, (Cured in Saturated Sand)		37.98	302	0.019	0.744	0.99	0.26
w/c=0.4, SMS=0.3% (Oven cured)	28 days	33.15	160	0.050	0.825	0.99	0.30
w/c=0.4, SMS=0.3% (Cured in Saturated Sand)		38.42	220	0.010	0.487	0.97	0.46

Figure 9. Compressive Piezoresistive Behavior of Smart Cement without and with Sodium Meta Silicate Addition after 1 Day Curing at 80°C Temperature

28 days of Curing

The compressive strength (σ_{cf}) of the smart cement after 28 days of curing at 80°C in the oven was 33.56 MPa which increased to 37.98 MPa when cured in the saturated sand at 80°C, a 13% increase. The smart cement with 0.3% SMS cured in oven had a compressive strength of 33.15 MPa which increased to 38.42 MPa when cured in saturated sand at 80°C, a 16% increase as summarized in Table 4.
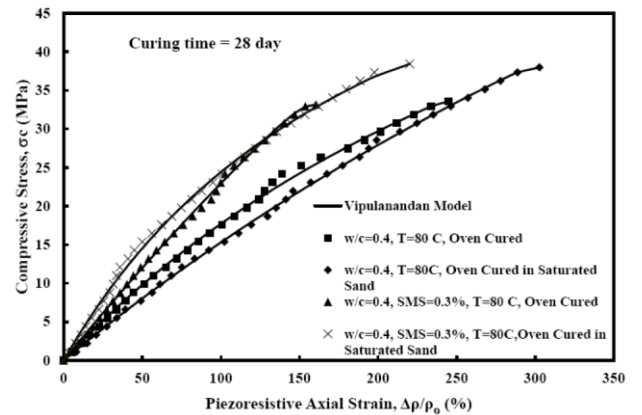

Figure 10. Compressive Piezoresistive Behavior of Smart Cement without and Sodium Meta Silicate Addition after 28 Days Curing at 80°C Temperature

The piezoresistive axial strain at failure $\left(\frac{\Delta\rho}{\rho_o}\right)_f$ for the smart cement cured at 80°C in the oven was 245% which increased to 302% when cured in the saturated sand at 80°C. The smart cement with 0.3% SMS cured in the oven at 80°C showed the piezoresistive axial strain at failure $\left(\frac{\Delta\rho}{\rho_o}\right)_f$ was 160% which increased to 220% for specimen cured in saturated sand at 80°C as summarized in Table 4. The piezoresistivity at the peak compressive stress varied from 900 to 1510 times the compressive strain of the smart cement.

Using the p-q piezoresistive model (Eqn. (4)), the relationship between the compressive stress and the piezoresistive axial strain $\left(\frac{\Delta\rho}{\rho_o}\right)$ of the smart cement with and without 0.3% SMS

for 28 days curing were modeled. The piezoresistive model (Eqn. (4)) predicted the measured stress-change in resistivity relationship very well as shown in Figure 10. The model parameters q_2 and p_2 are summarized in Table 4. The coefficients of determination (R^2) were 0.97 to 0.99. The root mean square of error (RMSE) varied between 0.26 MPa and 0.46 MPa as summarized in Table 4.

4.2.4 Modeling compressive strength with curing time

The compressive strength of the cement made with and without SMS and cured at 80°C in the oven and saturated sand was measured up to 28 days of curing. The compressive strength of the cement increased with the curing time in a non-linear manner as shown in Figure 11.
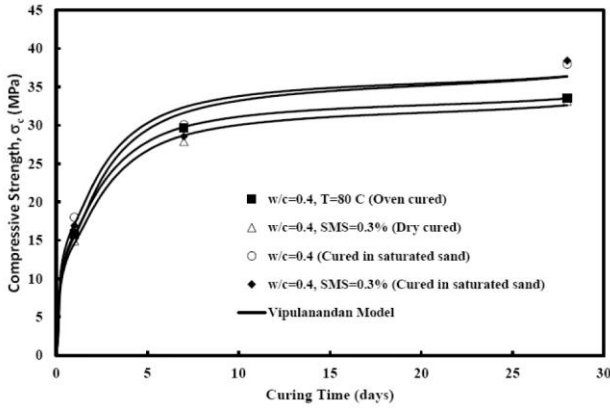

Figure 11. Variation of Compressive Strength of Smart Cement without and with Sodium Meta Silicate Addition up to 28 Days of Curing at 80°C Temperature

The relationship between the compressive strength of the cement and curing time was modeled with the Vipulanandan Correlation Model as follows:

$$\sigma_{cf} = t/(C_1 + D_1 t) \qquad (9)$$

Where,

σ_{cf} = Compressive strength of the smart cement (MPa)
t = Curing time (day)

Parameters C_1 (day/MPa) and D_1 (MPa^{-1}) are model parameters and parameter C_1 represent the initial rate of change and parameter D_1 determines the ultimate strength. For the cement cured at 80°C the oven, experimental results matched very well as shown in Figure 11 with the proposed model with coefficient of determination (R^2) of 0.99. For smart cement only, parameters C_1 and D_1 were found as 0.035 day/MPa and 0.028 MPa^{-1}. For smart cement with 0.3% SMS, parameters C_1 and D_1 were found as 0.039 day/MPa and 0.029 MPa^{-1}. For the cement cured in saturated sand at 80°C, experimental results also matched very well as shown in Figure 11 with the proposed model with coefficient of determination (R^2) of 0.94-0.95. For smart cement only, parameters C_1 and D_1 were found as 0.032 day/MPa and 0.026 MPa^{-1}. For smart cement with 0.3% SMS, parameters C_1 and D_1 were found as 0.038 day/MPa and 0.026 MPa^{-1}.

4.2.5 Modeling Piezoresistive Strain at Failure with Curing time

Piezoresistivity at failure for the smart cement made with and without SMS oven cured and cured up to 28 days was investigated. With curing time increases, the piezoresistivity at failure of the cement specimen changes. The relationship between the piezoresistivity at failure of the cement grout and curing time has been modeled using the Vipulanandan Correlation Model as follows:

$$\Delta\varrho/\varrho_o = (\Delta\varrho/\varrho_o)_1 - t/(E_1 + F_1 t) \qquad (10)$$

Where,

$\Delta\varrho/\varrho_o$ = piezoresistivity at failure (%)
$(\Delta\varrho/\varrho_o)_1$ = piezoresistivity at failure after 1 day (%)
t = Curing time (day)

Parameters E_1 (day/Ω.m) and F_1 (Ω.m)$^{-1}$ are model material parameters and the parameter E_1 represent the initial rate of change and the parameter F determines the ultimate piezoresistivity. For the cement cured at 80°C in the oven, the model predicted the experimental results very well as shown in Figure 12 with the coefficient of determination (R^2) were in the range of 0.98 to 0.99. For the oven dry cured smart cement, parameters E_1 and F_1 were 0.083 (day/Ω.m) and 0.0033 (Ω.m)$^{-1}$ respectively and the estimated ultimate piezoresistivity (infinite time) was over 130%. For the oven dry cured smart cement with 0.3% SMS, parameters E_1 and F_1 were found as 0.067 (day/Ω.m) and 0.0044 (Ω.m)$^{-1}$ respectively, and the estimated ultimate piezoresistivity (infinite time) was over 100%. For the cement specimens cured in saturated sand at 80°C, experimental results also matched very well shown in Figure 12 with the model with coefficient of determination (R^2) of 0.98-0.99. For smart cement cured in the saturated sand at 80°C, parameters E_1 and F_1 were 0.121 (day/Ω.m) and 0.0033 (Ω.m)$^{-1}$ respectively, and the estimated ultimate piezoresistivity (infinite time) was over 175%. For smart cement with 0.3% SMS cured in the saturated sand at 80°C, parameters E_1 and F_1 were found as 0.104 (day/Ω.m) and 0.0043 (Ω.m)$^{-1}$ respectively and the estimated ultimate piezoresistivity (infinite time) was over 120%.
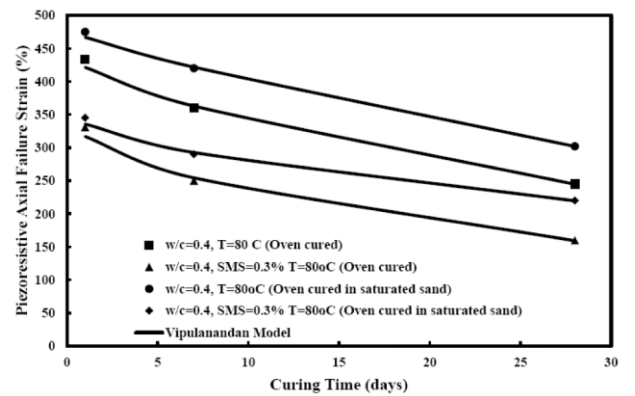

Figure 12. Variation of Piezoresistive Axial failure Strain of Smart Cement without and with Sodium Meta Silicate Addition up to 28 Days of Curing at 80°C Temperature

4.3. Effect of Clay Contamination

Portland cement slurries are not only used in the construction but also in repairing applications related to slurry walls, piles, other foundations, pipelines, tunnels, wells (oil, gas and

water), bridges, buildings and highways (McCarter et al. 2000; Fuller et al. 2002;; Vipulanandan et al. 2005 and 2014b; Wilson, 2017). Based on the applications, cement slurries are made with additives and water-to-cement ratios varying from 0.3 to over 1 (Nelson 1990; Vipulanandan et al. 2017). Construction of deep foundations, near surface structures and underground structures will require drilling in the ground using drilling muds and placing the cementitious materials in the boreholes may result in various types of clay soil contamination. Clay soil contamination will impact the cement hydration and long-term properties (Vipulanandan et al. 1995, 2018k). Unfortunately there are no real-time monitoring methods to detect the clay soil contamination of cementitious materials during construction and also the effects of clay contaminations during the service life of the infrastructures (Mohammed 2018; Vipulanandan et al. 2018k, 2020c).

Clay soils are mainly characterized as montmorillonite, kaolinite, illite or a mixture of these clay constituents with the particle sizes less than 2 ☐ m (Vipulanandan 1995a,b,2016f). Chemically the main constituent of the clay is aluminum silicates with vary amounts of cations such as sodium (Na), potassium (K), magnesium (Mg) and calcium (Ca) (Vipulanandan 1995; Mohammed et al. 2013 and 2015). Clays are hydrophilic inorganic materials which can react with both hydrating cement particles and the pore fluid. During drilling of boreholes to install water, oil and gas wells and drilled shafts to support bridges and buildings, water based drilling muds are used with varying amounts of bentonites clay contents (Vipulanandan 2014a). If the bore holes are not cleaned before placing the cement or concrete to construct drilled shafts the cement will get contaminated (Vipulanandan et al. 2018k). When installing oil and gas wells, after drilling is finished the metal casing is placed inside the wellbore and then the cement slurry is pumped through the casing so that it comes from bottom pushing the drilling mud and mud cake up and fills the gap between the casing and the formation (Wilson 2017). Also construction of tunnels in clay soils and shale rock formations could also contaminate the cement and concrete with clays. Flooding on construction sites will also result in contaminating the surfaces of the cementitious construction materials in-place by depositing transported clay sediments which will significantly impact the construction. Hence there is potential for the cement to be contaminated with clays from the drilling muds, mud cakes, flooding and the geological formations. Based on the type and the amount

contamination it will affect the performance of the cement and concrete (Vipulanandan 1995, 2014b, 2015c, 2018k).

The potential applications of smart cement with various types of chemical additives have been investigated under different curing conditions (temperatures, and saturated sand simulating the water saturated conditions in the bore holes) and the results are analyzed in this chapter to demonstrate the sensitivity of the chemo-thermo-piezoresistivity of the smart cements. Also the effects of clay (inorganic), oil based mud (organic) and carbon dioxide (CO_2) contaminations on the chemo-thermo-piezoresistive smart cement sensing characteristics were investigated.

4.3.1 Curing Methods

4.3.1.1 Room Condition

Specimens were cured in the plastic molds at room temperature (23oC) and a relative humidity of 50% and the specimens were demolded just before testing.

4.3.1.2 Oven Cured

Specimens were kept in the plastic mold and cured in the oven at elevated temperature. Also specimens were placed in saturated sand in the closed bottle (Figure 7) to simulate the field condition under water and groundwater and cured at room temperature and elevated temperatures and were demolded just before testing.

Also water was added regularly to keep the sand saturated.

4.3.2 Testing

In this study, the effects of up to 5% montmorillonite clay soil contamination on the initial properties and piezoresistive behavior of the Smart Portland cement was investigated. Smart Portland cement was made by mixing the cement (Type I) with 0.1% carbon fibers to enhance the sensing properties. Based on the type of construction, cement might get contaminated with varying amounts of clay soils. Hence, a series of experiments were performed to evaluate the cement behavior with and without up to 5% of montmorillonite clay contamination to determine the effects on the initial properties and the piezoresistivity with strength up to 28 days under room condition.

Table 5. Summary of the bulk resistivity parameters for the Smart Portland cement with and without clay soil contamination cured under room temperature up to 28 days

Mix Type	Unit Weight (kN/m³)	Initial resistivity, ϱ_o (Ω.m)	ϱ_{min} (Ω.m)	t_{min} (min)	ϱ_{24hr} (Ω.m)	$\varrho_{7\ days}$ (Ω.m)	$\varrho_{28\ days}$ (Ω.m)	$RI_{24\ hr}$ (%)	$RI_{7\ days}$ (%)	$RI_{28\ days}$ (%)
w/c=0.38	19.8	0.92	0.84	180	2.48	6.79	11.37	195	708	1253
w/c=0.38 Clay = 1%	19.5	0.94	0.85	180	2.62	6.57	12.30	208	673	1347
w/c=0.38 Clay = 5%	17.8	1.15	1.07	180	2.82	8.17	15.10	164	664	1311

4.3.2.1 Density

Initial unit weight of the smart Portland cement with w/c ratio of 0.38 was 19.8 kN/m³ as summarized in Table 5. The

initial unit weight decreased with the montmorillonite clay contamination. With 5% clay soil contamination, the unit weight decreased to 17.8 kN/m³, a 10% reduction.

4.3.2.2 Initial Resistivity

The initial resistivity of the modified Portland cement slurry was 0.92 Ω.m and it increased with the clay soil contamination as summarized in Table 5. With 1% clay soil contamination, the initial resistivity was increased to 0.94 Ω.m and with 5% clay soil contamination the initial resistivity was 1.15 Ω.m, a 25% increase. Hence the initial resistivity increases were more than two times more sensitive than the density changes of clay soil contamination in the cement.

4.3.2.3 Piezoresistivity and strength

1 day of curing

The compressive strength (σ_{cf}) of the smart Portland cement with 0%, 1%, and 5% clay soil contamination for one day of curing were 9.88 MPa, 9.44 MPa and 8.12 MPa, a 4%, and 18% reduction when the clay content was increased by 1% and 5% respectively as summarized in Table 6 and also shown in Figure 13.

The piezoresistive axial strain at failure $\left(\frac{\Delta\rho}{\rho_o}\right)_f$ for the modified Portland cement was 432% which was reduced to 411% and 230% respectively with 1% and 5% clay as summarized in Table 5. With 5% clay soil contamination to the smart Portland cement, the piezoresistive axial strain at failure $\left(\frac{\Delta\rho}{\rho_o}\right)_f$ was reduced about 45% from that of the smart Portland cement.

Using the p-q Piezoresistive model (Eqn. (4)), the relationships between compressive stress and the piezoresistive axial strain $\left(\frac{\Delta\rho}{\rho_o}\right)$ of the smart Portland cement with different clay content of 0%, 1% and 5% for one day of curing were modeled. The piezoresistive model (Eqn. (4)) predicted the measured stress-change in resistivity relationship very well as shown in Figure 13. The model parameters q_2 and p_2 are summarized in Table 5. The

coefficients of determination (R^2) were 0.97 to 0.99. The root mean square of error (RMSE) varied between 0.21 MPa and 0.43 MPa as summarized in Table 5.
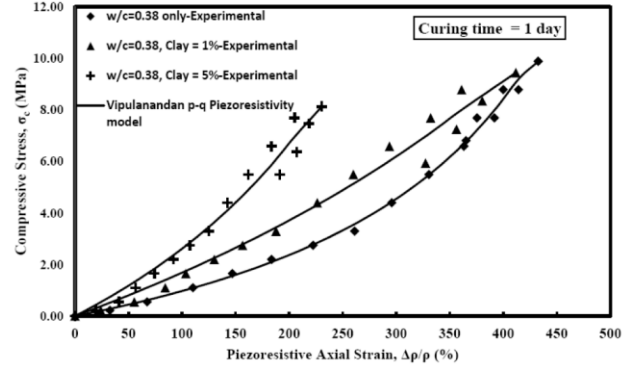

Figure 13. Compressive Piezoresistive Behavior of Smart Cement without and with Clay Contamination after 1 Day Curing

28 days of Curing

The compressive strength (σ_{cf}) of the modified Portland cement with 0%, 1%, and 5% clay soil contamination for one day of curing were 31.40 MPa, 30.08 MPa and 27.44 MPa, a 4%, and 13% reduction when the clay content increased about 1% and 5% respectively as summarized in Table 6 and also shown in Figure 14.

The piezoresistive axial strain at failure $\left(\frac{\Delta\rho}{\rho_o}\right)_f$ for the modified Portland cement was 270% which was reduced to 209% and 158% respectively with 1% and 5% clay as summarized in Table 6. With 5% clay soil contamination to the modified Portland cement, the piezoresistive axial strain at failure $\left(\frac{\Delta\rho}{\rho_o}\right)_f$ was reduced about 40% from that of the modified Portland cement.

Table 6. Compressive strength, piezoresistivity, model parameters p_2 and q_2 for the smart Portland Cement after 1 day and 28 days of curing.

Mix Type	Curing Time (day)	Strength σ_f (MPa)	Piezoresistivity at peak stress, $(\Delta\varrho/\varrho_o)_f$ (%)	p_2	q_2	R^2	RMSE (MPa)
w/c=0.38	1 day	9.88	432	0.047	2.77	0.99	0.21
w/c=0.38 Clay = 1%		9.44	411	0.025	1.48	0.98	0.43
w/c=0.38 Clay = 5%		8.12	230	0.031	1.64	0.97	0.43
w/c=0.38	28 days	31.40	270	0.062	0.75	0.98	0.44
w/c=0.38 Clay = 1%		30.08	209	0.052	0.75	0.99	0.34
w/c=0.38 Clay = 5%		27.44	158	0.125	0.78	0.99	0.34

Using the p-q Piezoresistive model (Eqn. (5.7)), the relationships between compressive stress and the piezoresistive axial strain $\left(\frac{\Delta\rho}{\rho_o}\right)$ of the modified Portland cement with different clay content of 0%, 1% and 5% for one day of curing were modeled. The piezoresistive model (Eqn.

(4)) predicted the measured stress- change in resistivity relationship very well as shown in Figure 14. The model parameters q_2 and p_2 are summarized in Table 6. The coefficients of determination (R^2) were 0.98 to 0.99. The root mean square of error (RMSE) varied between 0.34 MPa and 0.44 MPa as summarized in Table 6.
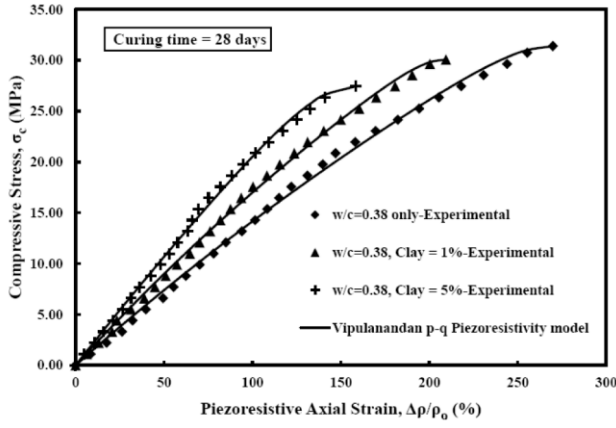
12

Figure 14. Compressive Piezoresistive Behavior of Smart Cement without and with Clay Contamination after 28 Days of Curing

4.3.2.4 Relationship between Curing Time and Strength and Piezoresistive Strain at Failure

The strength of the smart cement specimen made with and without clay soil contamination was measured up to 28 days of curing. With curing time increase, the compressive strength of the cement specimen increased.
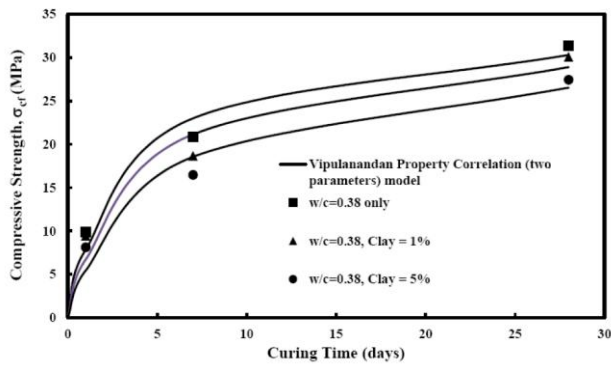

Figure 15. Variation of Compressive Strength of Smart Cement without and with Clay Contamination up to 28 Days of Curing at 80°C Temperature

The relationship between the compressive strength of the cement and curing time has been modeled with the Vipulanandan Property Correlation (two parameters since the initial condition is zero) model used for over two decades and the relationship is as follows:

$$\sigma_c = t/(C_2 + D_2 t) \qquad (11)$$

Where,

σ_c = Compressive strength of the grout (MPa)

t = Curing time (day)

Parameters C_2 and D_2 are model parameters and parameter C_2 represent the initial rate of change and parameter D_2 determines the ultimate strength. The experimental results matched very well as shown in Figure 15 with the proposed model with coefficient of determination (R^2) varied from 0.95 to 0.96. For smart Portland cement only, parameters C_2 and D_2 were found as 0.098 MPa^{-1}day and 0.029 MPa^{-1}. For the smart Portland cement with 1% clay, parameters C_2 and D_2

were 0.119 MPa^{-1}day and 0.030 MPa^{-1}. For the smart Portland cement with 5% clay, parameters C_2 and D_2 were 0.151 MPa^{-1}day and 0.032 MPa^{-1}.

4.3.2.5 Piezoresistive Failure Strain at Peak Stress

The piezoresistivity at peak failure stress for the cement specimen made with and without clay soil contamination were measured up to 28 days of curing. With the increase in curing time, the piezoresistivity at the peak failure stress for the cement reduced. The relationship between the piezoresistivity at failure of the cement and curing time has been modeled with the Vipulanandan Property Correlation model as follows:

$$\Delta\varrho/\varrho_o = (\Delta\varrho/\varrho_o)_2 - t/(E_2 + F_2 t) \qquad (12)$$

Where,

$\Delta\varrho/\varrho_o$ = Piezoresistivity at failure (%)

$(\Delta\varrho/\varrho_o)_2$ = Piezoresistivity at failure after 1 day (%)

t = Curing time (day)

Parameters E_2 and F_2 are model material parameters and parameter E_2 represent the initial rate of change and parameter F_2 determines the ultimate piezoresistivity. The experimental results matched very well as shown in Figure 16 with the proposed model with coefficient of determination (R^2) varied from 0.95 to 0.99. For modified Portland cement only, parameters E_2 and F_2 were found as 0.051 Ωm^{-1}day and 0.004 Ωm^{-1}. For modified Portland cement with 1% clay contamination, parameters E_2 and F_2 were found as 0.033 Ωm^{-1}day and 0.003 Ωm^{-1}. For modified Portland cement with 5% clay contamination, parameters E_2 and F_2 were found as 0.551 Ωm^{-1}day and 0.006 Ωm^{-1}.
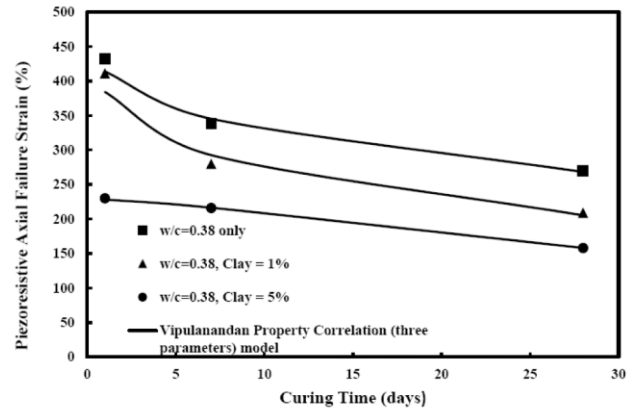

Figure 16. Variation of Piezoresistive Axial failure Strain of Smart Cement without and with Clay Contamination up to 28 Days of Curing

4.4. Carbon dioxide (CO$_2$) Contamination

The smart cement slurry was prepared with 1% and 3% of dry ice (CO$_2$) in water. The test specimens were prepared following the API standards. API class H cement was used with water-cement ratio of 0.38. For all the samples 0.04% (based on weight of cement) of carbon fiber (CF) was added to the slurry in order to enhance the piezoresistivity of the cement and to make it more sensing. After mixing, the slurries were casted into the cylindrical molds with height of 100 mm and diameter of 50 mm, with two conductive wires were embedded 50 mm apart vertically to monitor the resistivity

13

development of the specimens during the curing time. After 1 day all the specimens were demolded and were cured for 28 days under water.

4.4.1 Carbon dioxide (CO₂) Contamination

There is increasing interest in understanding the effects of carbon dioxide (CO_2) contamination of cement. In this study smart cement samples were prepared with CO_2 contaminated water by adding dry ice and also the cement specimens were cured in CO_2 contaminated water. Adding 3% of dry ice into the water reduced the temperature by about 3°C and also the pH and the resistivity ($\square$) as summarized in Table 7.

Table 7. Water with and without CO_2 Contamination

Solutions	pH	ρ $(\Omega.m)$
Pure Water	7.4	25.1
3% CO_2 in Water	4.2	22.3

Sample Preparation

The smart cement slurry was prepared with 0.1, 1 and 3% of dry ice (CO_2) in water. The test specimens were prepared following the API standards. API class H cement was used with water-cement ratio of 0.38. For all the samples, 0.04% (based on weight of cement) of carbon fiber (CF) was added to the slurry in order to enhance the piezoresistivity of the cement and to make it more sensing. After mixing, the slurries were casted into the cylindrical molds with height of 100 mm and diameter of 50 mm, with two conductive wires were embedded 50 mm apart vertically to monitor the resistivity development of the specimens during the curing time. After 1 day all the specimens were demolded and were cured for 28 days under water.

4.4.2 Testing

4.4.2.1 Density

The average density of smart cement was 1.95 g/cc (16.28 ppg). With 0.1% of CO_2 contaminated water the density reduced by 0.06%. With 1% of CO_2 contaminated water the density was reduced by 0.49% to 1.94 g/cc (16.20 ppg) and with 3% of CO_2 contaminated water it reduced to 1.93 g/cc (16.14 ppg), 0.86% reduction.

4.4.2.2 Electrical Resistivity

Initial resistivity

Initial resistivity of the smart cement slurries with varying CO_2 (dry ice) concentrations was investigated.

(a) Smart Cement: The average initial resistivity of the cement slurry was 1.10 Ω.m.

(b) Smart Cement with CO_2 Contamination: Smart cement with 0.1%, 1% and 3% of CO_2 contamination resulted in a reduction in the initial resistivity to 1.03 Ω.m, 0.93 Ω.m and 0.90 Ω.m respectively as summarized in Table 8. Hence, CO_2 contamination with concentrations of 0.1%, 1% and 3% resulted in the resistivity reduction of 6%, 15% and 18% respectively. The main reason for the reduction in initial electrical resistivity of the contaminated cement slurries was due to the existence of carbonic acid (H_2CO_3) in the slurries.

Curing

During the initial period of curing the resistivity will reduce with time. Also the time to reach the minimum resistivity will be also a good monitoring parameter and it is important to quantify the sensitivity of these parameters due to CO_2 contamination.

(a) Smart Cement: The minimum resistivity of the smart cement slurry was 0.85 Ω.m and was reached 85 minutes (t_{min}) after mixing the sample (Table 8).

(b) CO_2 Contaminated Smart Cement: CO_2 contamination decreased the ρ_{min} of the smart cement slurry by 7%, 15% and 17% from 0.85 Ω.m to 0.79 Ω.m, 0.72 Ω.m and 0.70 Ω.m respectively with 0.1%, 1% and 3% of CO_2 contamination. CO_2 exposure also delayed the hydration process. With 0.1%, 1% and 3% of CO_2 contamination it delayed t_{min} by 15 minutes, 35 minutes and 45 minutes respectively.

One Day Curing

The test results are summarized in Table 8.

(a) Smart Cement: After one day of curing the smart cement resistivity was 4.8 Ω.m and the resistivity index was 465%

Table 8. Electrical resistivity parameters of the smart cement slurries exposed to different CO_2 concentration

Smart Cement	ρ_0 $(\Omega.m)$	ρ_{min} $(\Omega.m)$	t_{min} $(minute)$	ρ_{24} $(\Omega.m)$	$\dfrac{\rho_{24} - \rho_{min}}{\rho_{min}}$ %
Uncontaminated cement	1.10	0.85	85	4.80	465%
0.1% CO_2 Contaminated Smart Cement	1.03	0.79	100	4.20	432%
1% CO_2 Contaminated Smart Cement	0.93	0.72	120	3.80	428%
3% CO_2 Contaminated Smart Cement	0.90	0.70	130	3.30	371%

(b) CO_2 Contaminated Smart Cement: CO_2 contamination reduced the development of the resistivity during the one day of curing. The 0.1%, 1% and 3% of CO_2 contaminated resistivity after one day of curing were 4.20 , Ω.m 3.80 Ω.m and 3.30 Ω.m respectively. Also the contamination reduced the resistivity indices as summarized in Table 8.

28 Days Curing

(a) Smart Cement: After 28 days of curing the smart cement resistivity was 17.0 Ω.m.

(b) CO_2 Contaminated Smart Cement: CO_2 contamination reduced the development of the resistivity during the 28 days

of curing. The 0.1%, 1% and 3% of CO_2 contaminated cement reduced the resistivity of the cement by 21%, 34% and 38% to 13.4 Ω.m, 11.3 Ω.m and 10.5 Ω.m respectively after 28 days of curing.

4.4.2.3 Compressive Strength

Compressive behavior of smart cement was tested after 1 and 28 days of curing under water at room temperature as shown in Figure 17.
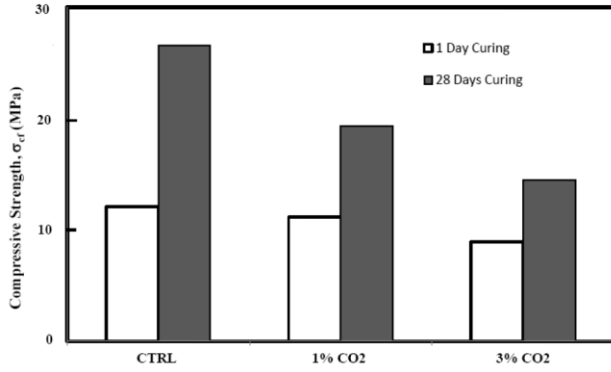

Figure 17. Variation of Compressive Strength of Smart Cement without and with Clay Contamination up to 28 Days of Curing at 80°C Temperature

1 day curing

(a) Smart Cement: The compressive strength of the smart cement was 12.5 MPa (1.81 ksi) after1 day of curing.

(b) CO_2 Contaminated Smart Cement: CO_2 contamination decreased the compressive strength of the smart cement. The compressive strength of the smart cement contaminated with 1% and 3% of CO2 decreased to 11.5 MPa (1.67 ksi) and 9.2 MPa (1.34 ksi) respectively, 8% and 26% reduction after 1 day of curing.

28 days of curing

(a) Smart Cement: The compressive strength of the smart cement after 28 days of curing under water was 27.5 MPa (3.98 ksi).

(b) CO_2 Contaminated Smart Cement: The compressive strength of the smart cement contaminated with 1% and 3% of CO_2 decreased by 27% and 45% respectively to 20.0 MPa (2.90 ksi) and 15.0 MPa (2.17 ksi) after 28 days of curing.

4.4.2.4 Piezoresistivity

Stress-piezoresistive strain behavior of smart cement was evaluated after 28 days of curing under water using Vipulanandan p-q piezoresistive strain softening model (Eqn. 5.6) and shown in Figure 18.
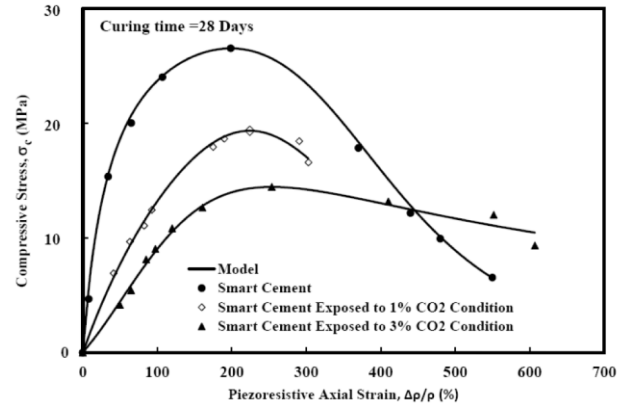

Figure 18. Compressive Piezoresistive Behavior of Smart Cement without and with CO_2 Contamination up to 28 Days of Curing

28 days curing

(a) Smart Cement: After 28 days of curing, the piezoresistivity of the smart cement was 199%. The model parameters p_2 and q_2 were 0.45 and 0.15 respectively as summarized in Table 9.

(b) CO_2 Contaminated Smart Cement: CO_2 contamination increased the piezoresistive behavior of the smart cement as shown in Figure 18. Piezoresistivity of the smart cement contaminated with 1% CO_2 was 224% at the failure, a 13% increase. The p-q model parameters p_2 and q_2 for the 1% CO2 contaminated smart cement were 0.35 and 0.47 respectively. Piezoresistive strain at failure of the smart cement contaminated with 3% CO_2 was 254% at the failure, a 28% increase. The p-q model parameters p_2 and q_2 for the 3% CO_2 contaminated smart cement were 0.15 and 0.76 respectively as summarized in Table 9.

Table 9. Piezoresistive Model parameters for the smart cement contaminated with CO_2 after 28 days of curing

Materials	28 Days Curing				Compressive Strength (MPa)	Piezoresistivity at Failure (%)
	p_2	q_2	R^2	RMSE (MPa)		
Smart Cement	0.45	0.15	0.99	0.49	27.5	199
1% CO2 + Smart Cement	0.35	0.47	0.98	0.68	20.0	224
3% CO2 + Smart Cement	0.15	0.76	0.99	0.52	15.0	254

5. REAL-TIME MONITORING

5.1 New Construction

Highly sensing smart cement and smart cement concrete can be used in many applications. But it is important to monitor the curing and performance of the smart materials.

5.1.1 Two Probe Wireless Transmissions

It is important to monitor the changes in the resistivity (material property) with time to ensure the quality of the mixed material and also curing under various environmental conditions. It has been proven that two probe method with alternative current (AC) supply can be used for monitoring the changes in resistivity and the schematic of the

configuration is shown in Figure 19(a). A company named Sensytec located in Houston, Texas has developed the wireless transmission monitoring probe including a thermocouple to monitor the temperature as shown in Figure 19(b). The measurements can be wirelessly transmitted to the phone. The probes can be place in concrete beams, column, slabs and other configuration to monitor the curing and also the stress developments in the smart cement, smart concrete, regular concrete and cement elements.
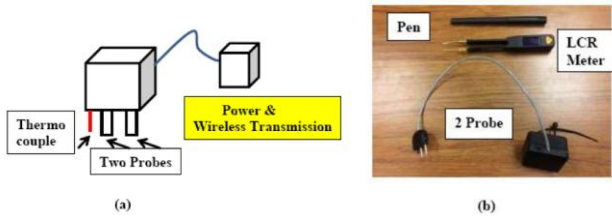

Figure 19. Two Probe Monitoring with Wireless Transmission (a) Schematic and (b) Actual Device (SensyRoc), two probe pocket LCR and a Pen.

5.1.2 New Wells (Oil, Gas and Water)

One of the main focuses is to develop real-time monitoring systems for the field wells which could be several thousand feet in the ground to collect data from the field wells during the installation and the entire service life of the wells. Also ways to integrate the LCR meter monitoring system into the current field monitoring systems to collect the data from the smart cement. This can eliminate the failures and also minimize the losses.

5.1.3 Field Instrumentation

The main focus will be to integrate the two probe method to monitor the performance of the smart drilling fluids, smart spacer fluids, smart cement and smart packer fluids during various stages operations. During the drilling, the two probes will be part of the drilling tool where the smart drilling fluid conditions could be monitored with depth using the AC current at relatively high frequency of about 300 kHz. When casing is lowered into the well, it can be used as a probe with a floating ring on the surface on the fluid as the second probe. The casing couplings will have selected frequency **"Band-Pass Filter"** attached to represent various depths (Figure 20). The **Band-Pass filters** (BPF) are simple device designed using resistances and capacitors to be effective in a selected range of frequency (Kureve et al. 2014; Zhang et al. 2015). When AC current is passed through the casing in the selected frequency range (Figure 20), it will get to the depth of the compatible filter and the filter will allow that range of frequency to pass through to the cement to measure the vertical resistance between the selected casing ring with the filter and the floating ring on the top of the liquid. Studies have clearly indicated that the current will only pass through the cement since the resistance is the lowest compared to the resistance of the steel-cement interface and cement-geological formation interface. Also when the current is passed through the casing from the top, it will only get to the cement through the compatible frequency "Band-Pass Filter" since the interface resistance between the cement and steel are very large. For example, if 50 to 100 kHz AC current is applied at the top of the casing current will travel through to Level 4 and will be allowed to get to the cement at that level.

It will then travel to the floating probe ring at the top and the Impedance – Frequency data collected in this region can be used to determine the resistance (CASE 2) and using the parameter K, the resistivity can be determined.
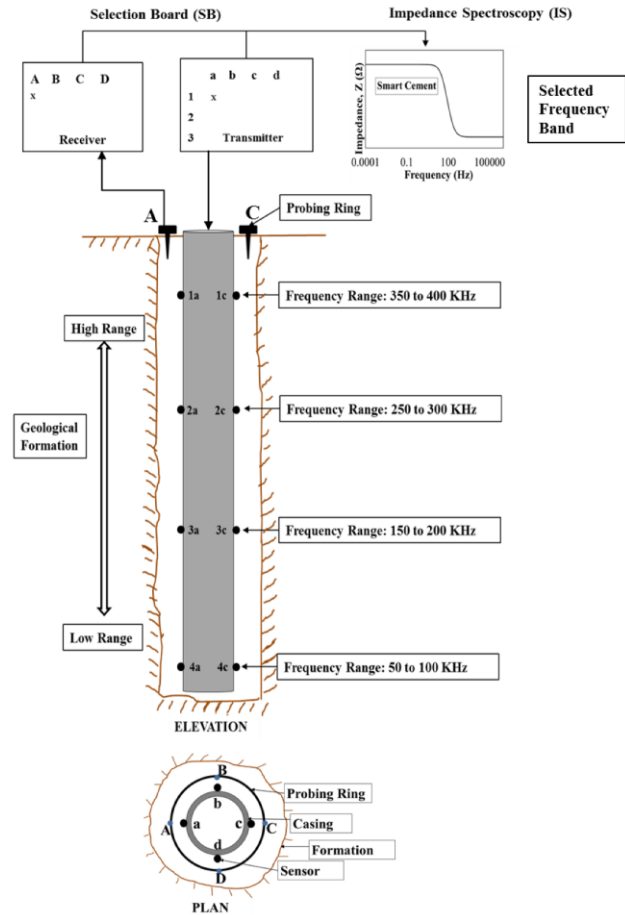

Figure 20. Schmatic Configration of the Field Wells to be Installed

5.1.4 Processing and Analyses of Data:

Computer software will be developed to rapidly process the collected data to display it on the monitoring screen real-time. Models used to characterize the material properties including resistivity will be used. The display will focus on displaying the resistivity with time, rate of change of resistivity with time $(d\rho/dt)$ and the second derivative of resistivity change $(d^2\rho/dt^2)$ with time (three parameters) as shown in Figure 21. Based on the quantification, limits on the rate of changes in resistivity and second derivative of resistivity change will be established and used as guidance to evaluate the conditions in the well. When no limits are exceeded (three parameters) the operation is fine that there will be **No Warning** (green light will be on). When all three parameters are beyond the limit then there will be **High Warning** (Red Light). Also based on the understanding of the changes in the three parameters the causes of the problems will be listed, so the operator can do the needed modification. When one parameter is exceeded there will be **Low Warning** (Yellow Light) and the causes will be identified based on the parameter violated. When two parameters are exceeded there will be **Medium Warning** (Orange Light) and the causes will be identified based on the two parameters violated the operators can the find t methods to fix the problem.
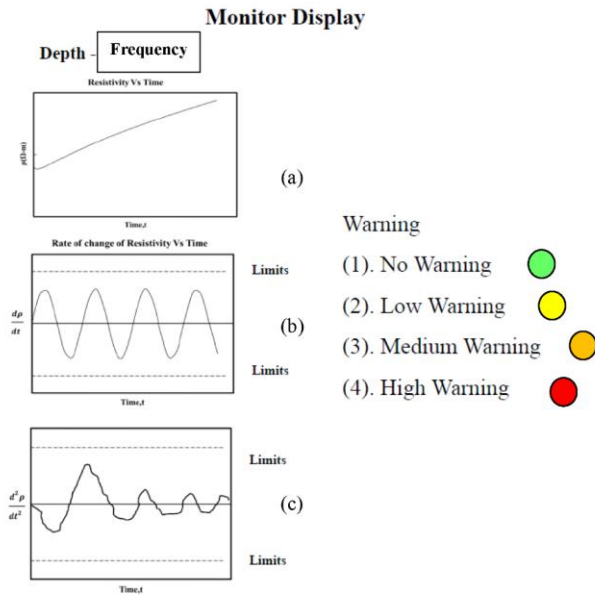
Figure 21. Variation of Total and Rates of Electrical Reisistivity with Tme at Various Depths
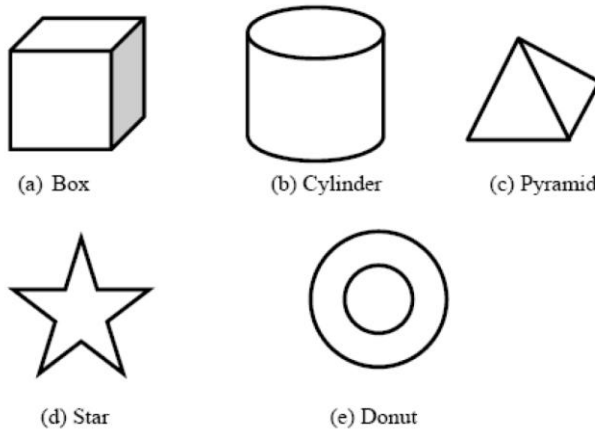

Figure 22. Diffenent Smart Cement and Smart Concrete Block Configuration

5.2 In-service Infrastructures

With the advancement of the new smart cement technology it is important to develop methods to integrate it with infrastructures that are in-service. This can substantial improve the current maintenance operations and also minimize failures. Also the developed methods should be relatively easy to adopt with various infrastructures.

In Figure 22, smart cement and smart concrete integrated with the two-probe monitoring system can be made into different shapes of blocks and attached at the critical locations of the the infrastructures that are in service. The resistivity and temperature can be measured in these blocks and transmitted wirelessly.

6. CONCLUSIONS

Main focus was to experimentally verifying the chemo-thermo-piezoresistive behavior of the smart cement. The effect of aggregate addition (concrete) with the smart cement binder was investigated. In order to evaluate the chemical (chemo) sensitivity of the smart cement with an inorganic

additive (sodium meta silicate) and inorganic and organic contaminants (clay, CO_2-carbon dioxide) were tested. Also, the effect of temperature and the curing environments (oven and saturated sand) on the smart cement behavior was investigated with and without the sodium meta silicate additive. Based on the experimental study and analytical modelling following conclusions are advanced:

- Addition of coarse aggregate and curing time increased the initial electrical resistivity of the smart cement composite as well as long term electrical resistivity. The initial electrical resistivity of smart cement was 1.02 Ω.m which increased to 3.74 Ω.m. with 75% gravel respectively. After 28 days of curing, the electrical resistivity of smart cement was 14.14 Ω.m which increased to 61.24 Ω.m. with 75% gravel respectively. Also Vipulanandan Curing Model predicted the electrical resistivity development in th concrete very well.

- The piezoresistivity of the smart cement with 0% and 75% gravel content after 28 days of curing were 204% and 101% at a peak compressive stress respectively. Vipulanandan Piezoresistivity Model can be used to predict the piezoresistivity behaviour of the smart cement concrete very well.

- The failure strain of concrete is 0.3%, hence piezoresistive concrete has magnified the monitoring resistivity parameter by 336 times (33,600%) or more higher based on the aggregate content and making the concrete a bulk sensor.

- Silicate additive (inorganic) and contaminants (organic and inorganic) including CO_2 (organic) used in this study changed the density and initial resistivity of the smart cement. All the changes in the resistivity have been quantified. The smart cement with the additives and contaminants was highly sensing chemo-piezoresistive cement.

- Also the effect of temperature on the smart cement with and without sodium silicate was investigated and the smart cement was thermo-piezoresistive.

- The monitoring parameter, electrical resistivity was highly sensitive to the type and amount of additive and contaminants compared to the other parameters such as density and strength. Also resistivity can be monitored in the field during the entire service life of the smart cement.

- Effects of contaminants such as clay (inorganic) and CO_2 solution (organic) on the mechanical properties and piezoresistive behaviour of the smart cement was tested and quantified.

- Vipulanandan p-q curing model and piezoresistive model predicted the experimental results very well based on the root mean square error (RMSE) and coefficient of determination.

- The relationship between the changes in the compressive strengths of the smart cement with the curing time have been modelled with the Vipulanandan

Property Correlation model and the experimental values matched very well with the model predictions based on coefficient of determination and RMSE. The relationship between the piezoresistivity at failure and curing time was also modeled with the Vipulanandan Property Correlation model and the predictions agreed very well with the experimental results.

- Real-time 2- Probe monitoring system with wireless transmission of the data to the phone has been developed and can be easily used in the field.

- In deep wells, band pass filters (BPF) can be integrated with the casing coupling to do the real-time monitoring. This approach can be adopted for deep foundations and pipelines.

- Smart cement and smart cement concrete blocks integrated with wireless real-time monitoring can be adopted in the in-service infrastructures for real- time monitoring for improved maintenance and minimize failure.

Acknowledgements

Declaration

There is no conflict of interest. No ethical issues. Agree to publish this paper.

REFERENCES

Afolabi, R. Esther O. Yusuf, E. Chude V. Okonji, C. and Nwobodo, S. (2019), "Predictive Analytics for the Vipulanandan Rheological Model and its Correlative Effect for Nanoparticle Modification of Drilling Mud," Journal of Petroleum Science and Engineering, Vol. 183, pp. 1-10.

ASTM C136 (2016). Standard Test Method for Sieve Analysis of Fine and Coarse Aggregates. ASTM International, West Conshohocken, PA.

Carter, K. M. and Oort, E. (2014), Improved Regulatory Oversight Using Real- Time Data Monitoring Technologies in the Wake of Macondo, SPE 170323, pp. 1-51.

Chung, D. D. L (1995), "Strain Sensors Based on Electrical Resistance Change," Smart Materials Structures, No. 4, pp. 59-61.

Chung, D. D. L., (2000) "Cement Reinforced with Short Carbon Fibers: A Multifunctional Material," Composites, Part B, Vol. 31, 2000, pp. 511–526. (1

Chung, D.D.L (2001), "Functional Properties of cement-Matrix Composites," Journal of Material Science, Vol. 36, pp. 1315-1324.

CIGMAT CT 3-06, (2006), "Standard Test Method for Bonding Strength of Coatings and Mortars: Sandwich Mehod," Center for Innovative Grouting Materials and Technology (CIGMAT), University of Houston, Houston, Texas, U.S.A.

CIGMAT CT 1-06, (2006), "Standard Test Method for Chemical Resistance of Coated or Lined Concrete and Clay Bricks," Center for Innovative Grouting Materials and Technology (CIGMAT), University of Houston, Houston, Texas, U.S.A.

CIGMAT PC 1-02, (2002), "Standard Practice for Making and Curing Polymer Concrete Test Specimens in Laboratory," Center for Innovative Grouting Materials and Technology (CIGMAT), University of Houston, Houston, Texas, U.S.A.

CIGMAT GR 2-02 (2002), "Standard Test Methods for Unconfined Compressive Strength of Grouts and Grouted Sands," Center for Innovative Grouting Materials and Technology (CIGMAT), University of Houston, Houston, Texas, U.S.A.

Davies, R. J., Almond, S., Ward, R. S., Jackson, R. B., Adams, C., Worrall, F., Whitehead, M. A. (2014). Oil and gas wells and their integrity: Implications for shale and unconventional resource exploitation. Marine and Petroleum Geology, 56, 239-254.

Eoff, L. and Waltman, B. (2009) "Polymer Treatment Controls Fluid Loss While Maintaining Hydrocarbon Flow, Journal of Petroleum Technology, pp. 28-30.

Fuller, G., Souza, P., Ferreira, L., and Rouat, D. (2002). "High-Strength Lightweight Blend Improves Deepwater Cementing," Oil & Gas Journal, Vol. 100, No.8, pp. 86-95.

Hou, T. C., Su, Y. M., Chen, Y. R. and Chen, P. J. (2017). Effects of coarse aggregates on the electrical resistivity of Portland cement concrete. Construction and Building Materials, 133, 397-408.

Izon, D. and M. Mayes, M. (2007) "Absence of fatalities in blowouts encouraging in MMS study of OCS incidents 1992-2006," Well Control Magazine, pp. 86-90.

Kureve, T. D., Mise, G. A. and Atsuwe, B. (2014) "Implementation of An Active RC band-Pass Filter at Varying Quality Factors Using Matlab, International Journal of Scientific and Technology Research, Vol. 3, No. 5 pp. 350-352.

Labibzadeh, M., Zhhabizadeh, B. and Khajehdezfuly, A., (2010) "Early Age Compressive Strength Assessment of Oil Well Class G Cement Due to Borehole Pressure and Temperature Changes, Journal of American Science, Vol. 6, No.7, pp.38-47.

Mbaba, P.E. and Caballero, E.P. 1983. "Field Application of an Additive Containing Sodium Metasilicate During Steam Stimulation". Proceeding-SPE Annual Technical Conference and Exhibition, San Francisco, California, 5-8 October, 1983.

McCarter, W. J., Starrs, G. and Chrisp, T. M. (2000). Electrical conductivity, diffusion, and permeability of Portland cement-based mortars. Cement and Concrete Research, 30(9), 1395-1400.

Mohammed, A. S. (2018). Vipulanandan model for the rheological properties with ultimate shear stress of oil well

cement modified with nanoclay. Egyptian journal of petroleum, 27(3), 335-347.

Montes, D., Orozco, W., Tabora, E.A., Franco, C. A. and Cortes, F.B. (2019) "Development of Nanofluids for Perdurability in Viscosity Reduction of Extra-Heavy Oils," MDPI , Energies 2019, Vol. 12, 1068, doi:10.3390/en12061068, MDPI.

Nelson, E.B., 1990. "Well Cementing." Elsevier Science BV, Amsterdam, The Netherlands, 1990, 3-10.

Parvasi, S. M., Xu, C., Kong, Q. and Song, G. (2016). Detection of multiple thin surface cracks using vibrothermography with low-power piezoceramic-based ultrasonic actuator—a numerical study with experimental verification. Smart Materials and Structures, 25(5), 055042.

Princigallo, A., van Breugel, K. and Levita, G. (2003). Influence of the aggregate on the electrical conductivity of Portland cement concretes. Cement and Concrete Research, 33(11), 1755-1763.

Siemens, W. (1871) "On the Increase in Electrical Resistance in Conductors with Rise of Temperature and its Applications to Measure the of Ordinary and Furnace Temperatures, Also simple Method of Measuring Electrical Resistance," The Bakerian lecture, Royal Society, Retrieved May 14, 2014.

Smith, C.S. (1954), "Piezoresistive Effect in Germanium and Silicon," Physical Review, Vol. 94, pp. 42-49.http://dx.doi.org/10.1102/PhysRev. 94.42.

U.S. Patent Number 10,481,143 Awarded on November 19, 2019, "Chemo-thermo—piezoresisitive highly sensing smart cement with integrated real-time monitoring system" Inventor: C. Vipulanandan - International Patent App. PCT/US2016/041905, 2016 ;(WO2017022460).

Vipulanandan, C. and Paul, E., 1990. "Performance of Epoxy and Polyester Polymer Concrete" ACI Materials Journal, Vol. 87, No. 3, May-June, 1990, p. 241-251.

Vipulanandan, C., and Shenoy, S., 1992. "Properties of Cement Grouts and Grouted Sands with Additives." Proceeding-ASCE Specialty Conference on Grouting, Soil Improvement and Geosynthetics, pp. 500-511.

Vipulanandan, C. and Liu, J. (2002). "Film Model for Coated Cement Concrete." Cement and Concrete Research, Vol. 32(4), 1931-1936.

Vipulanandan, C., and Liu, J. (2005a) "Polyuretane Based Grouts for Deep Off-Shore Pipe-in-Pipe Application", Proceedings, Pipelines 2005, ASCE, Houston, TX, pp. 216-227.

Vipulanandan, C. and Ortega, R.(2005b) Editors, Proceedings, Pipelines 2005, Design, Optimization and Maintenance in Today's Economy, ASCE, Houston, TX, 2005, 1149 p.

Vipulanandan, C. and Townsend, F. C.(2005c) Editors, Proceedings, Advances in Designing and Testing Deep Foundations, ASCE, GSP 129, Austin, TX, 2005, 347 p.

Vipulanandan, C. and Townsend, F. C (2005d) Editor, Proceedings, Advances in Deep Foundations, ASCE, GSP 132, Austin, TX, 2005.

Vipulanandan, C., and Liu. J. (2005e) "Sewer-Pipe Joint Infiltration Test Protocol Developed by CIGMAT ", Proceedings, Pipelines 2005, ASCE, Houston, TX, pp. 553-563, August 2005.

Vipulanandan, C., and Garas, V. (2006), "Piezoresistivity of Carbon Fiber Reinforced Cement Mortar", Proceedings, Engineering, Construction and Operations in Challenging Environments, Earth & Space 2006, Proceedings ASCE Aerospace Division, League City, TX, CD-ROM.

Vipulanandan, C. (2007a) Editor, Proceedings, Advances in Measurement and Modeling of Soil Behavior, ASCE, GSP 173, Denver Colorado, 2007.

Vipulanandan, C., and Kulkarni, S. P. (2007b) "Shear Bonding and Thermal Properties of Particle-Filled Polymer Grout for Pipe-in-Pipe Application," Journal of Materials in Civil Engineering , Vol. 19, No. 7, pp.583-590.

Vipulanandan, C. and Garas, V. (2008). Electrical resistivity, pulse velocity, and compressive properties of carbon fiber-reinforced cement mortar. Journal of Materials in Civil Engineering, 20(2), 93-101.

Vipulanandan, C., Dimrican, E., and Harendra, S. (2010), "Artificial Neural Network and Nonlinear Models for Gelling and Maximum Curing Temperature Rise in Polymer Grouts," Journal of Materials in Civil Engineering, Volume 23, No. 4, p. 1-6.

Vipulanandan, C. and Prasanth, P., (2013)" Impedance Spectroscopy Characterization of a piezoresistive Structural Polymer Composite Bulk Sensor," Journal of Testing and Evaluation, Vol. 41, No.6, 898-904.

Vipulanandan et al. (2014a), "Development and Characterization of Smart Cement for Real Time Monitoring of Ultra-Deepwater Oil Well Cementing Applications, OTC-25099-MS.

Vipulanandan et al. (2014b), "Characterization of Smart Cement Modified with Sodium Meta Silicate for Ultra-Deepwater Oil Well Cementing Applications, AADE-14-NTCE-03.

Vipulanandan, C. Heidari, M., Qu, Q., Farzam, H., and Pappas, J. M. (2014c), "Behaviour of piezoresistive smart cement contaminated with oil based drilling mud," Offshore Technology Conference, OTC 25200-MS, pp. 1-14.

Vipulanandan, C. and Mohammed, A. (2014d), "Hyperbolic rheological model with shear stress limit for acrylamide polymer modified bentonite drilling muds," Journal of Petroleum Science and Engineering, 122, 38–47.

Vipulanandan, C., and Mohammed, A., (2015a) "Smart cement rheological and piezoresistive behavior for oil well applications." Journal of Petroleum Science and Engineering, V-135, 2015, pp. 50-58.

Vipulanandan, C., and Mohammed, A., (2015b) "Smart cement modified with iron oxide nanoparticles to enhance the piezoresistive behavior and compressive strength for oil well applications." Journal of Smart Materials and Structures, Vol. 24 Number 12, pp. 1-11.

Vipulanandan, C, Krishnamoorti, R. Mohammed, A., G. Narvaez, Head, B. and Pappas, J. (2015c) "Iron Nanoparticle Modified Smart Cement for Real Time Monitoring of Ultra Deepwater Oil Well Cementing Applications", Offshore Technology Conference (OTC) 2015, OTC-25842-MS.

Vipulanandan, C, Ramanathan, P. Ali, M., Basirat, B. and Pappas, J. (2015d) "Real Time Monitoring of Oil Based Mud, Spacer Fluid and Piezoresistive Smart Cement to Verify the Oil Well Drilling and Cementing Operation Using Model Tests", Offshore Technology Conference (OTC) 2015, OTC-25851-MS.

Vipulanandan, C. and Ali, K. (2016a) "Smart Cement Piezoresistive Behavior with and without Sodium Meta-silicate Under Temperature and Curing Environments for Oil Well Applications," Journal of Civil Engineering Materials, American Society of Civil Engineers (ASCE), doi 10.1061/MT.1943-055330001667.

Vipulanandan, C., Ali, K., Basirat, B., A. Reddy, Amani, N., Mohammed, A. Dighe, S., Farzam, H. and W. J. Head (2016b), "Field Test for Real Time Monitoring of Piezoresistive Smart Cement to Verify the Cementing Operations ," Offshore Technology Conference (OTC), OTC-27060-MS.

Vipulanandan, C., and Mohammed, A., (2017) "Rheological Properties of Piezoresistive Smart Cement Slurry Modified With Iron Oxide Nanoparticles for Oil Well Applications." Journal of Testing and Evaluation, ASTM, Vol. 45 Number 6, pp. 2050-2060.

Vipulanandan, C., Mohammed, A. and Ganpatye, A. (2018a) "Smart Cement Performance Enhancement with NanoAl2O3 for Real Time Monitoring Applications Using Vipulanandan Models," Offshore Technology Conference (OTC), OTC-28880-MS.

Vipulanandan, C., and Ali, K., (2018b) "Smart Cement Grouts for Repairing Damaged Piezoresistive Cement and the Performances Predicted Using Vipulanandan Models" Journal of Civil Engineering Materials, American Society of Civil Engineers (ASCE), Vol. 30, No. 10, Article number 04018253.

Vipulanandan, C., and Amani, N., (2018c) "Characterizing the Pulse Velocity and Electrical resistivity Changes In Concrete with Piezoresistive Smart Cement Binder Using Vipulanandan Models" Construction and Building Materials, Vol. 175, pp. 519-530.

Vipulanandan, C., and Mohammed, A., (2018d) "Smart Cement Compressive Piezoresistive Stress-Strain and Strength Behavior with Nano Silica Modification, Journal of Testing and Evaluation, ASTM, doi 10.1520/JTE 20170105.

Vipulanandan, C. (2021) Smart Cement: Development, Testing, Modeling and Real-Time Monitoring, Taylor and Francis CRC Press, pp. 402.

Vipulanandan, C and Maddi, A.R.(2021) Characterizing the thermal, piezoresistive, rheology and fluid loss of smart foam cement slurries using artificial neural network and Vipulanandan Models, Journal of Petroleum Science and Engineering, Vol. 207.

Wilson, A. 2017. "Real-Time Monitoring of Piezoresistive Smart Cement to Verify Operations," SPE, Journal of Petroleum Technology (JPT), pp. 79-80.

Wohltjen, H., Barger, W.R. Snow, A.W. and Jarvis, N. L. (1985) "A vapor-sensitive chemiresistor fabricated with planar microelectrodes and Langmuir-biodegett organic semiconductor film," IEE Transaction Electron Devices, 32 (7), pp. 1170-1174.

Zhang, M., Sisomphon, K., Ng, T.S, and Sun, D.J, (2010a). "Effect of superplasticizers on workability retention and initial setting time of cement pastes," Construction and Building Materials 24, 1700–1707.

Zhang, J., Weissinger, E.A, Peethamparan, S, and Scherer, G.W., (2010b). "Early hydration and setting of oil well cement," Cement and Concrete research, Vol. 40, 1023-1033.

Zhang, M. Zhang, F. and Luo, X. (2015), "Design of Miniaturized Band Pass Filter with Composite Right/Left-handed Transmission Line," Journal of Computer and Communications, Vol. 3, pp. 44-48.